

## Performance of conventional and modified solar photovoltaic array configuration under the combined effect of seasonal variation and partial shaded conditions

Niti Agrawal \* 

University of Delhi, Shyamlal College, Department of Physics, Delhi-110032, India,  
nagrawal@shyamlal.du.ac.in

Submitted: 28.07.2024

Accepted: 23.01.2025

Published: 31.03.2025



\* Corresponding Author

**Abstract:** The energy yield of the photovoltaic (PV) array varies with every season, primarily due to variation in the availability of solar insolation and ambient temperature. Moreover, the energy generation of an installed PV array gets severely impacted by the partial shading conditions (PSCs), which occurs when neighbouring objects or even debris cast shadow on some portion of the array. The combined effect of seasonal variation and partial shading can lead to more pronounced fluctuation and deterioration in the energy yield of the PV array. In this work, the performance of a conventional and modified PV array configuration under the combined effect of seasonal variation and PSC has been investigated. Both the array configurations have been characterized experimentally in real field conditions under uniform and PSCs. The outdoor current-voltage (I-V) data and weather data is used to estimate the seasonal energy yield and DC performance ratio of the arrays under different PSC scenarios. It is found that under unshaded condition, both the PV arrays generate same energy in different seasons. Under PSCs, the modified PV configuration outperforms the conventional one, with a notable improvement in energy generation in all the seasons.

**Keywords:** Array, Energy yield, Partial shading, Performance ratio PV

Cite this paper as: Agrawal N., Performance of conventional and modified solar photovoltaic array configuration under the combined effect of seasonal variation and partial shaded conditions. *Journal of Energy Systems* 2025; 9(1): 52-67, DOI: 10.30521/jes.1523575

2025 Published by peer-reviewed open access scientific journal, JES at DergiPark (<https://dergipark.org.tr/jes>)

## 1. INTRODUCTION

Conventional resources of energy are depleting at an accelerated rate and are also major contributor to the alarming environment pollution. To overcome the adverse impact of these conventional energy resources, and meet the ever-growing demand of energy the focus has now been shifted to renewable energy resources such as solar, wind, hydro etc. Among the various renewable energy generation technologies, solar photovoltaic (SPV) is the most important and has gained attention as it is bountiful, clean, has low prices etc. In the last decade, the total installed SPV capacity has increased from 72 GW to 707 GW [1]. SPV is a simple process of conversion of solar energy into electrical energy directly using solar cells. Many solar cells are connected together to form a PV module, which are further interconnected to constitute solar PV arrays.

Despite many positive features of SPV, when a PV array is installed in the field, it faces many obstacles in delivering maximum power and its efficiency of energy generation often becomes uncertain. This is because the SPV energy yield in the field is determined by the local operating conditions rather than standard test conditions (STC) of temperature 25°C, solar irradiance 1000 W/m<sup>2</sup> and AM1.5G spectrum [2,3]. Various conducted studies have demonstrated that the PV output performance exhibits a pronounced seasonal variation [4,5,6,7,8]. This is attributed mainly due to change in solar irradiance, spectral content, ambient temperature wind speed with different seasons [9,10,11,12]. Solar irradiance and ambient temperature are crucial factors which plays the fundamental role in determining the energy yield of a solar PV system. The available solar insolation and ambient temperature varies across seasons, resulting in variation in the performance of PV array with seasons. Alexander 2015 studied the seasonality and performance loss rates of 11 grid connected photovoltaic systems of different technology. Their studies showed that DC performance ratio (PR) of SPV is different in different seasons. The PR of crystalline silicon technology was found to be higher during winters and low during summers. Vashisht 2016 evaluated the capacity utilization factor and PR of a 20 kWp solar plant under different seasons and climatic conditions of India. Their study highlighted the correlation of PR of a SPV to its behavior in different seasons, with module temperature as the key factor of comparison. Along with seasonal variation, weather conditions like clouds or haze can also affect the solar irradiance levels. However, the nature of this problem may vary with geographical location. The available annual solar radiation and ambient temperature at each location in turn directly influences the annual energy demand [13].

Additionally, there is one more condition which hinders the incident solar irradiance non uniformly and can significantly affect the energy generation of the PV array, even under favorable environmental conditions. This condition is known as partial shading conditions (PSCs), which arise when the shadow of any nearby structure or building, surrounding vegetation, debris etc. falls on some portion of the installed PV array. Even when the PV modules have optimum tilt and orientation as per the geographical location, shading from the surroundings becomes unavoidable [14]. Usually, it is very difficult to shift or remove objects in the neighborhood of PV system casting shadow over it. Under such conditions, some portions of the PV array's surface are shaded repeatedly, on daily basis unless the source causing partial shading is removed or rectified. Such reiterated partial shadings can seriously deteriorate the PV array's energy yield [15,16,17]. Researchers have focused extensively on modifying conventional array configurations to maximize output power from partially shaded PV arrays [18]. Accordingly, literature presents various types of static configurations such as series (S), parallel (P), series-parallel (SP), bridge linked (BL), honey comb (HC), total cross tied (TCT) (Fig.1) [19,20,21,22,23]. Pendem and Mikkili, (2018) compared these configurations of array size 5x5 under different shading scenarios such as uneven row, uneven column, diagonal, random, short and narrow, short and wide, long and narrow, and long and wide shading patterns [19]. The authors found that TCT configuration shows least mismatching losses due to PSC. Bingöl and Özkaya, (2018) also compared the performance of different configurations of a larger array size of 6x6 under six different shading cases [20]. The obtained results

show that TCT has the lowest mismatch loss under PSCs. Also, advanced or hybrid configurations [24,25], mathematical puzzle based [26,27,28] and PV reconfiguration techniques [29,30] have also been tested and compared using different methodologies. However, the comparison of different configurations is based on their instantaneous output power at a specific operating temperature and irradiance (generally 25°C and 1000 W/m<sup>2</sup>).

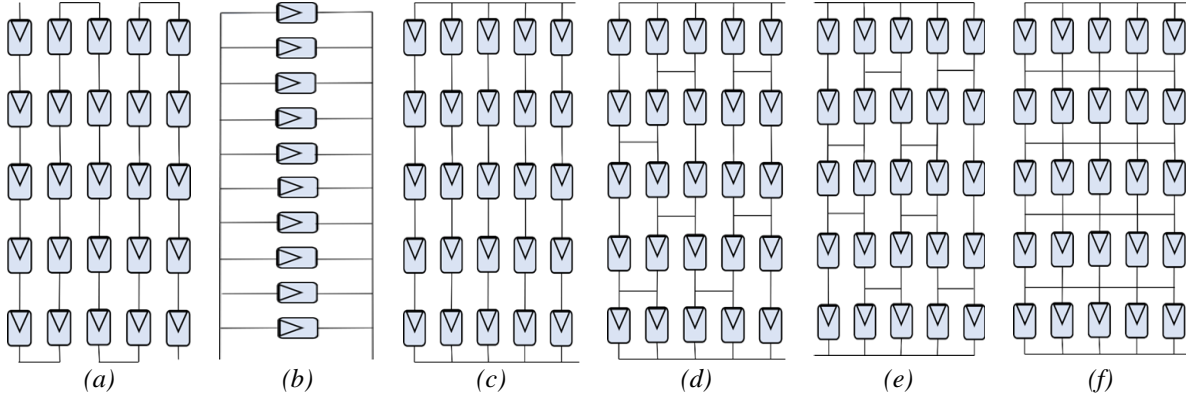


Figure 1. Array configurations: (a) Series, (b) parallel, (c) series parallel, (d) bridge linked, (e) honey comb, (f) total cross tied.

But, the installed PV array experience wide range of solar irradiance, ambient temperature, and other conditions like partial shadings, the energy yield and performance ratio (PR) of a PV array becomes crucial performance parameters. They provide insights into how well a PV array configuration can perform and endure the adverse effects of persistent partial shading and other environmental conditions [15].

As discussed above, the energy yield of a PV system is influenced strongly by the seasonal variation and additionally if PSCs exist, more pronounced fluctuations in PV energy output are obtained. Since the viability of a PV array installation can be assessed primarily by its energy generation, understanding its variations is crucial for predicting and optimizing the PV energy output. The author in this paper presents the experimental study to estimate and compare the energy yield and DC PR of two different configurations of PV array under the combined effect of seasonal variation and PSCs. The two PV arrays used are conventional S-S array and modified TCT-S array (details are presented in section 2). I-V data for both the PV arrays have been obtained experimentally in real field conditions under uniform and partial shading conditions. Using the outdoor I-V data of PV arrays, data for local solar irradiance, ambient temperature, wind speed and translation equations present in the literature, seasonal energy yield and DC performance ratio of both the PV arrays have been estimated. In this study, five seasons which are prevalent in India (spring, summer, monsoon, post monsoon and winter) and three PS conditions - horizontal, vertical and square shaped have been considered. It is investigated how the long-term performance of a PV array is impacted under the combined impact of seasonal variation and PSCs, and how these parameters can be improved by modifying the conventional architecture of the PV array.

Studying the energy yield of solar panels in different seasons under PSC is important for optimizing their performance. Shading can significantly reduce energy production, and understanding how this varies across seasons helps in designing more efficient systems. It allows for the development of strategies to minimize the energy yield variations and deterioration such as panel placement, tilt angles, or modifying the PV configuration to mitigate shading effects and maximize overall energy output.

## 2. METHODOLOGY

This section briefly describes the various steps of the methodology used for this study. Further details of the methodology are presented in [31].

**STEP I: Selecting PV array configurations**

In this study, two different configurations of PV array have been used, as described below:

1. Conventional Configuration: This is series in series or S-S array configuration. This configuration of PV array is formed by connecting S-modules in series. S-module is the one which has 36 PV cells connected in series, the schematic of which is shown in Fig. 2(a).
2. Modified Configuration: This is total cross tied in series or TCT-S Array configuration. In this configuration, TCT-modules are connected in series to form the TCT-S PV array [18]. TCT modules is the one in which 36 constituent PV cells are interconnected in TCT scheme, the schematic of which is presented in Fig. 2(b).

**STEP II: Measuring outdoor I-V data of PV array configurations**

All measurements for the PV arrays were conducted at the National Institute of Solar Energy (NISE) in Gurugram, Haryana, India. The site is located at a latitude of 28.4700° N, a longitude of 77.0300° E, and an elevation of 216 meters above sea level. Both the arrays were mounted on rigid structures with a tilt angle of 28.5°, facing south. For measuring the outdoor I-V data of the arrays, Solmetric P-V Analyzer (PVA-1000S), was used.

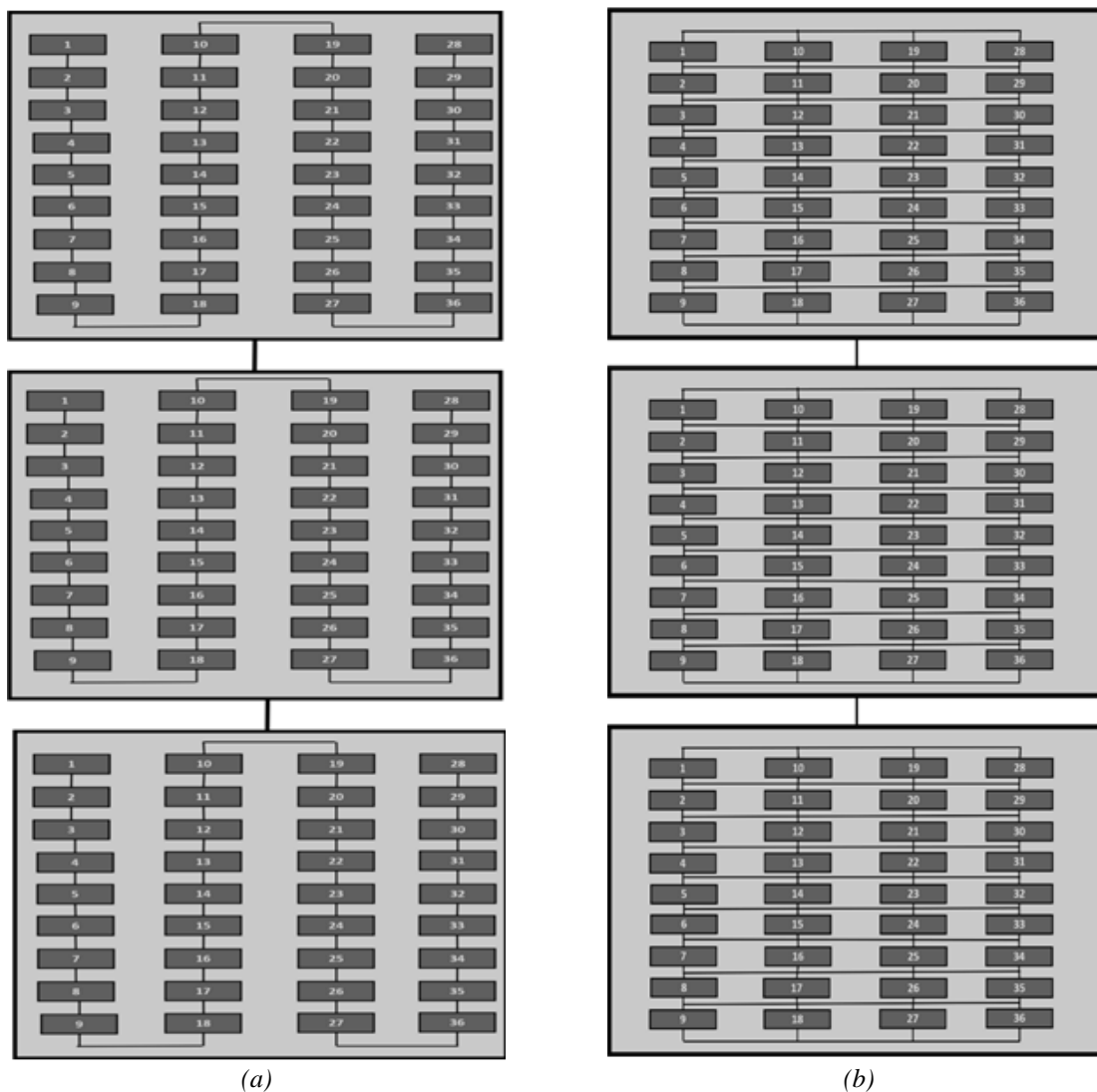


Figure 2. Schematic of (a) conventional S-S, (b) modified TCT-S PV array configurations.



(1) (2) (3)  
 Figure 3. Shading scenarios used in the study (1) horizontal (2) vertical and (3) square shaped.

**STEP III: Creating partial shading conditions**

Three PSCs, namely horizontal, vertical and square shaped shading patterns have been generated artificially using paper sheets, as shown in Fig. 3.

**STEP IV: Generating power matrix ( $P_{max}$ )**

Using the collected outdoor  $I-V$  data for both the arrays, the 22-element  $P_{max}$  matrix was generated in accordance with IEC61853-1 [32]. The  $P_{max}$  matrix consist of 22 conditions of different temperature and irradiance as presented in Table 1. A total of eight such  $P_{max}$  matrices have been generated corresponding to both the PV arrays under uniform irradiance condition, horizontal, vertical and square shaped shading condition.

Table 1.  $P_{max}$  at 22 sets of Irradiance and Temperature Conditions as per IEC 61853-1 standard [32].

| <b><math>P_{max}</math> versus Irradiance and Temperature</b> |                         |    |    |    |
|---|-------------------------|----|----|----|
| Irradiance (W/m <sup>2</sup> )                                | Module Temperature (°C) |    |    |    |
|   | 15                      | 25 | 50 | 75 |
| 100   | 1                       | 2  | NA | NA |
| 200   | 3                       | 4  | NA | NA |
| 400   | 5                       | 6  | 7  | NA |
| 600   | 8                       | 9  | 10 | 11 |
| 800   | 12                      | 13 | 14 | 15 |
| 1000  | 16                      | 17 | 18 | 19 |
| 1100  | NA                      | 20 | 21 | 22 |

**STEP V: Collecting weather data**

The data for local solar irradiance ( $G$ ), ambient temperature ( $T$ ) and wind speed ( $WS$ ) was recorded after every 10 minutes, for one complete year. The instruments used for these measurements are EKO, MS-802 pyranometer, Young, 05103 wind sensor and Vaisala, HMP 155 Vaisala, HMP 155 temperature sensor respectively. The obtained solar radiation (kWh/m<sup>2</sup>) and average temperature of the season is presented in Fig. 4

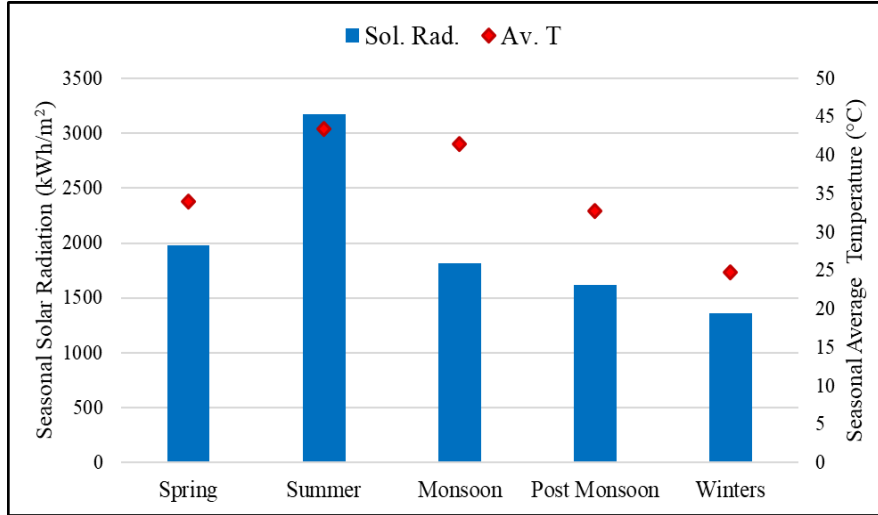


Figure 4. Obtained solar radiation (kWh/m<sup>2</sup>) and average temperature (°C) in different seasons in a year.

**STEP VI: Estimating PV array operating temperature**

The operating temperature of the array is estimated using Eq. (1) [33].

$$T_a = G(e^{a+bWS}) + T, \quad (1)$$

where,  $T_a$  and  $T$  are the back-surface array temperature and ambient air temperature in (°C),  $G$  is the Solar irradiance incident on module surface, (W/m<sup>2</sup>),  $WS$  is the measured wind speed (m/s), and  $(a)$ ,  $(b)$  are empirically found coefficients having value of -3.56 and -0.0750, respectively [33].

**STEP VII: Segregating data in different irradiance bins**

The obtained annual irradiance data is segregated in the seven bins corresponding to seven irradiance conditions mentioned in  $P_{max}$  matrix.

**STEP VIII: Identifying reference conditions of irradiance, temperature and power corresponding to the weather data**

To estimate the instantaneous power generated by any array under any particular condition i.e., uniform irradiance or any one of the shading conditions, the experimentally generated  $P_{max}$  matrix by the array under that scenario is becomes the reference matrix. Corresponding to each instantaneous measured value of irradiance and array temperature, the closest conditions of irradiance and temperature from the  $P_{max}$  matrix is selected as the reference irradiance ( $G_{ref}$ ) and temperature ( $T_{ref}$ ) conditions. Under the  $G_{ref}$  and  $T_{ref}$  conditions, the power generated by the array ( $P_{ref}$ ) is obtained from the  $P_{max}$  matrix. Similarly, the reference conditions of  $G_{ref}$ ,  $T_{ref}$  and  $P_{ref}$  are identified from the obtained  $P_{max}$  matrix for all the recorded instantaneous weather conditions for the entire year.

**STEP IX: Estimating instantaneous power corresponding to the weather data**

The instantaneous power output ( $P_o$ ) corresponding to the measured data of  $G$  and  $T_a$  (every 10 minutes) is estimated using the following translation equations [34]:

For  $G > 125$  W/m<sup>2</sup>,

$$P_o = \left(\frac{G}{G_{ref}}\right) P_{ref} \left((T_a - T_{ref}) \gamma + 1\right) \quad (2)$$

for  $G \leq 125 \text{ W/m}^2$ ,

$$C_p = \left( \frac{G^2 0.008}{G_{ref}} \right) P_{ref} ((T_a - T_{ref}) \gamma + 1) \quad (3)$$

Where, ' $\gamma$ ' is the temperature coefficient of power in (% /°C).

The seasonal power generation of the array is obtained by adding the instantaneous power obtained for that period.

**STEP X: Estimation of seasonal energy yield and performance ratio**

For the comparison of the seasonal energy yield and DC performance ratio, a normalized rating of 1kW for S-S and TCT-S array has been considered in this study. Five different seasons which are prevalent in India have been considered: Spring (Feb-March), summer (April-June), monsoon (July-Sep), post monsoon (Oct-Nov) and winter (Dec-Jan).

Energy yield of the PV array ( $E_o$ ), under any condition of uniform irradiance or partial shaded condition, is estimated using Eq. (4) given below:

$$C_p = (\Delta t) \Sigma P_{oi}, \quad (4)$$

where,  $\Delta t$  represents data sampling interval of 10 minutes and  $P_{oi}$  is the estimated instantaneous power output of the array at the  $i$ th sample time (W). DC Performance ratio (PR) is the ratio of measured output to expected output for a given period based on the system name-plate rating and is calculated according to the Eq. (5) given below [35]:

$$PR = \frac{(E_o/P_{STC})}{(H_i/G_{STC})}, \quad (5)$$

where,  $E_o$  is the PV energy output (D.C) in kWh,  $P_{STC}$  is the array power rating (D.C) at STC in kW,  $H_i$  is the total in-plane irradiation in kWh/m<sup>2</sup> and  $G_{STC}$  is the solar irradiance at STC (= 1000 W/m<sup>2</sup>)

### 3. RESULTS AND DISCUSSION

#### 3.1 For Unshaded Outdoor Condition

Using the methodology described earlier, the seasonal energy yield and DC performance ratio is estimation for both the arrays firstly under no shadow condition. The estimated energy generation for S-S and TCT-S array for different seasons is presented in Table 2. The annual estimated energy yield of S-S and TCT-S array is 1544.0 kWh and 1540.2 kWh respectively.

Table 2. Energy generation of 1kW each of S-S and TCT-S configuration in different seasons under unshaded condition.

| Season              | Energy Generation under unshaded condition (kWh) |        | Performance Ratio under unshaded condition |       |
|---------------------|--|--------|--|-------|
|                     | S-S  | TCT-S  | S-S  | TCT-S |
| Spring              | 314.2  | 313.5  | 0.958                                      | 0.961 |
| Summer              | 479.3  | 472.7  | 0.903                                      | 0.893 |
| Monsoon             | 282.4  | 282.4  | 0.929                                      | 0.926 |
| Post Monsoon        | 254.4  | 256.3  | 0.945                                      | 0.958 |
| Winter              | 213.8  | 215.3  | 0.937                                      | 0.948 |
| <b>Annual Yield</b> | 1544.0   | 1540.2 | 0.928                                      | 0.923 |

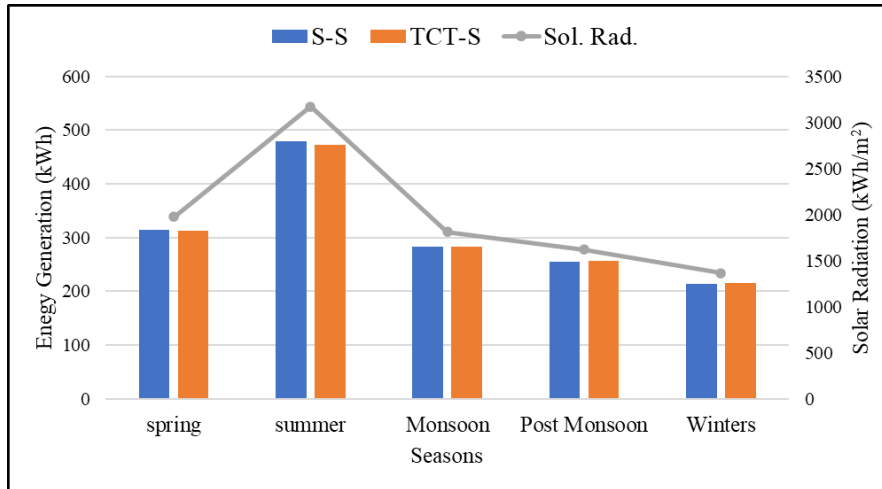


Figure 5. Variation in the energy yield for S-S and TCT-S array and received solar radiation in different seasons.

The variation in the energy yield for both the arrays and incident solar radiation with different seasons is presented in Fig. 5. It is evident from the obtained results that out of the five seasons, the energy yield for both the arrays is maximum in the month of summer (479.3 kWh for S-S and 472.8 kWh for TCT-S), followed by spring, monsoon, post monsoon season and minimum in winters (213.8 kWh for S-S and 215.3 kWh for TCT-S). This is because the solar radiations received in this year is also maximum in summer followed by spring, monsoon, post monsoon season and minimum in winters.

The estimated percentage of the total annual energy generated in different seasons is presented in Fig. 6. Maximum percentage of the annual energy (31.0%) is generated in summer season while minimum (14.0%) is generated in winter season.

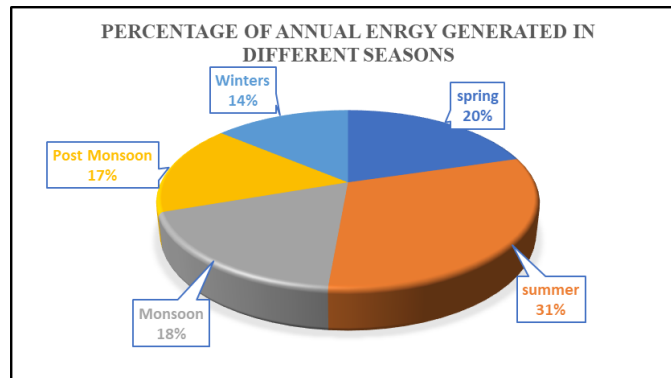


Figure 6. Percentage distribution of annual energy generated in different seasons under unshaded condition.

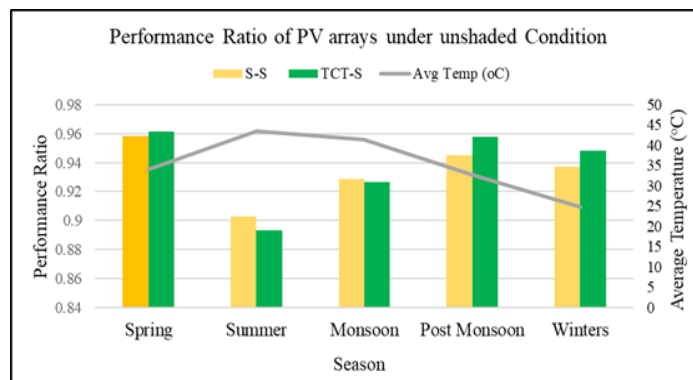


Figure 7. DC performance ratio of S-S and TCT-S array under unshaded condition and average temperature obtained in different seasons in a year.

The variation of the estimated DC Performance Ratio (PR) and average temperature with seasons is presented in Fig. 7. PR of the array varies in different seasons. The maximum PR is obtained in spring season followed by post monsoon, winter and monsoon, and least in summer. It is seen that, as the temperature increases PR of the PV array decreases. The highest temperature obtained in summer results in lowest PR, in spite the fact that maximum percentage of the annual energy is generated in summer.

It is to be noted that the minor difference in the obtained energy generation and DC performance ratio of both the arrays under uniform irradiance conditions can be attributed to the manufacturer’s tolerance in electrical characteristics of constituent cells/modules.

### 3.2 Scenario-1: Horizontal Shading

#### 3.2.1 Power output of the arrays under horizontal shading

The surface plot representing the variation of average  $P_{max}$  with different conditions of irradiance and temperature under horizontal shading is presented Fig. 8. The obtained values of  $P_{max}$  for S-S array ranges from 20 W to 648 W, while for TCT-S array it is from 22 W to 757 W. The power output of S-S and TCT-S array at 1000 W/m<sup>2</sup> and 25 °C is 513.4 W and 656.0 W respectively.

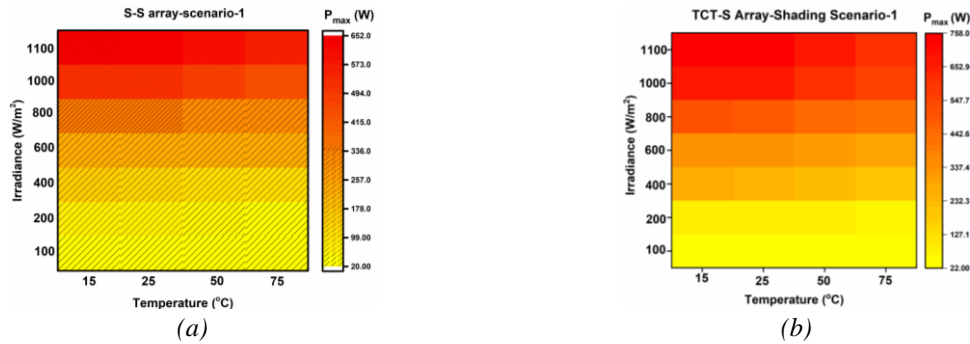


Figure 8. Surface plot showing the variation of  $P_{max}$  with irradiance and temperature under shading scenario-1 for (a) S-S and (b) TCT-S array.

#### 3.2.2 Energy yield and DC performance ratio under horizontal shading

The estimated total energy generated in one year by S-S and TCT-S array is 658.4 kWh and 864.2 kWh respectively. The seasonal energy yield and DC PR of both the arrays under the impact of horizontal shading is presented in Table 3. As seen from the results, seasonal energy yield and DC PR of the arrays is significantly reduced w.r.t the unshaded case.

The seasonal energy loss for S-S array ranges from 125.8 kWh in winters (58.8% loss) to 270.5 kWh in summer (56.4% loss). For TCT-S array, the energy loss ranges from 98.7 kWh in winters (45.8% loss) to 197.3 kWh in summer (41.7% loss). On an average, S-S array suffers an energy loss of 57.6% while for TCT-S it is reduced to 44.3%.

Table 3. Seasonal energy generation by array and DC performance ratio of 1kW each of S-S and TCT-S configuration under the impact of horizontal shading.

| Season       | Energy Generation under horizontal shading (kWh) |       | Performance Ratio under horizontal shading |       |
|--------------|--|-------|--|-------|
|              | S-S  | TCT-S | S-S  | TCT-S |
| Spring       | 138.5  | 183.6 | 0.420                                      | 0.552 |
| Summer       | 208.7  | 275.4 | 0.387                                      | 0.487 |
| Monsoon      | 118.1  | 148.5 | 0.386                                      | 0.504 |
| Post Monsoon | 105.1  | 140.1 | 0.393                                      | 0.513 |
| Winter       | 88.0   | 116.6 | 0.393                                      | 0.511 |

The estimated PR of the PV arrays also fluctuate with the seasons. The highest PR is obtained in spring season (0.420 for S-S and 0.552 for TCT-S) and least in summer (0.386 for S-S and 0.487 for TCT-S). The average yearly PR of S-S array falls to ~ 0.39, whereas for TCT-S array it is ~ 0.52.

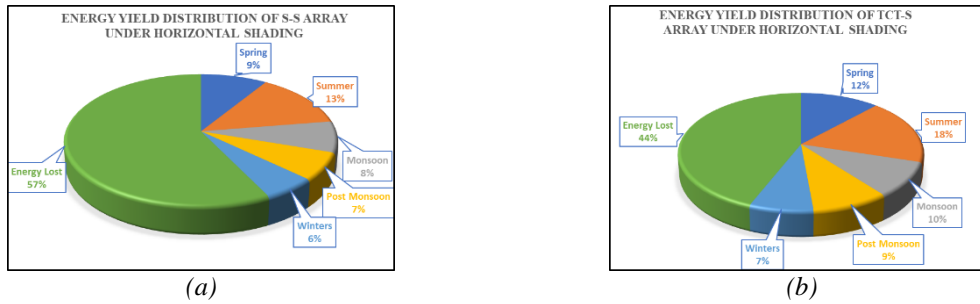


Figure 9. Percentage distribution of energy generated (%) and lost (%) in different seasons under the impact of horizontal shading w.r.t the unshaded condition: (a) S-S and (b) TCT-S arrays.

The energy generated (%) and lost (%) in different seasons under the impact of horizontal shading w.r.t the unshaded condition is presented in Fig. 9. Under this shading condition, maximum energy generated by both the arrays is still in summer season. However, the energy generation is reduced to 13.5% for S-S and 17.9% for TCT-S array, in comparison to 31% generated in summer season under unshaded condition. Out of all the seasons, minimum energy is generated in winter, 5.7% for S-S and 7.6% for TCT-S in comparison to 14% energy generated in winter season under unshaded condition.

### 3.3 Scenario-2: Vertical Shading

#### 3.3.1 Pmax matrix generated under vertical shading

The surface plot representing the variation of average  $P_{max}$  with different conditions of irradiance and temperature under horizontal shading is presented Fig. 10. Under the impact of vertical shading, the obtained values of  $P_{max}$  for S-S array ranges only from 13.9 W to 634.0 W, while for TCT-S array it is from 50.5 W to 991.0 W. The power output of S-S and TCT-S array at 1000 W/m<sup>2</sup> and 25 °C is 504.2 W and 866.1 W respectively.

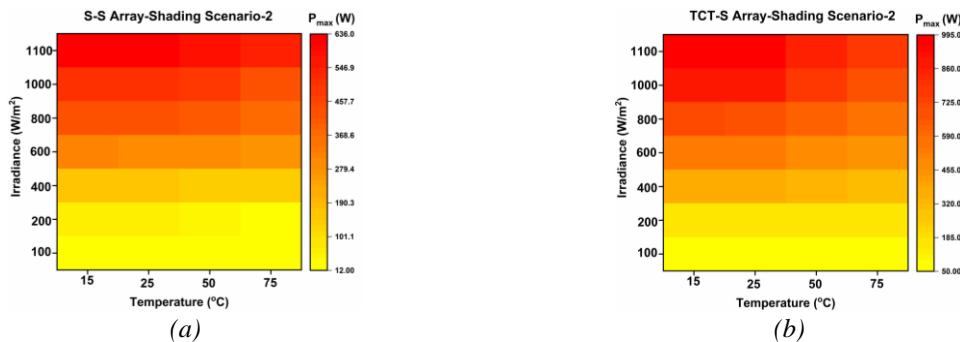


Figure 10. Surface plot showing the variation of  $P_{max}$  with irradiance and temperature under shading scenario-2 for (a) S-S and (b) TCT-S arrays.

#### 3.3.2 Energy yield and DC performance ratio under vertical shading

The total energy generated in one year by S-S and TCT-S array is 775.8 kWh and 1339.5 kWh respectively. The seasonal energy yield and DC PR of both the arrays under the impact of vertical shading is presented in Table 4. As seen from the results, w.r.t unshaded case, seasonal energy yield and DC PR of the S-S is significantly reduced for S-S and only a little for TCT-S array.

Table 4. Seasonal energy generation by array and DC performance ratio of 1kW each of S-S and TCT-S configuration under the impact of vertical shading.

| Season       | Energy generation under vertical shading (kWh) |       | Performance ratio under vertical shading |       |
|--------------|--|-------|--|-------|
|              | S-S  | TCT-S | S-S                                      | TCT-S |
| Spring       | 159.9  | 273.6 | 0.486                                    | 0.827 |
| Summer       | 246.2  | 413.7 | 0.450                                    | 0.771 |
| Monsoon      | 139.9  | 244.0 | 0.464                                    | 0.791 |
| Post Monsoon | 127.2  | 222.1 | 0.470                                    | 0.818 |
| Winter       | 107.6  | 186.0 | 0.471                                    | 0.807 |

The seasonal energy loss for S-S array ranges from 106.2 kWh in winters (50.0% loss) to 233.0 kWh in summer (56.4% loss). For TCT-S array, the energy loss ranges from 29.3kWh in winters (13.1% loss) to 59.0 kWh in summer (12.5% loss). On an average, S-S array suffers an energy loss of 49.7% while TCT-S array exhibits much-reduced energy loss of only 13 %, under shading scenario-2.

As seen from the obtained results, the highest PR for S-S array obtained is 0.486 (in spring season) and least is 0.450 in summer. On an average, PR of S-S array falls to 0.486 under this shading scenario-2. For TCT-S array, highest PR obtained is 0.827 and least is 0.771 in spring and summer seasons respectively. On an average, PR obtained for TCT-S array is 0.803, nearly double that of S-S array.

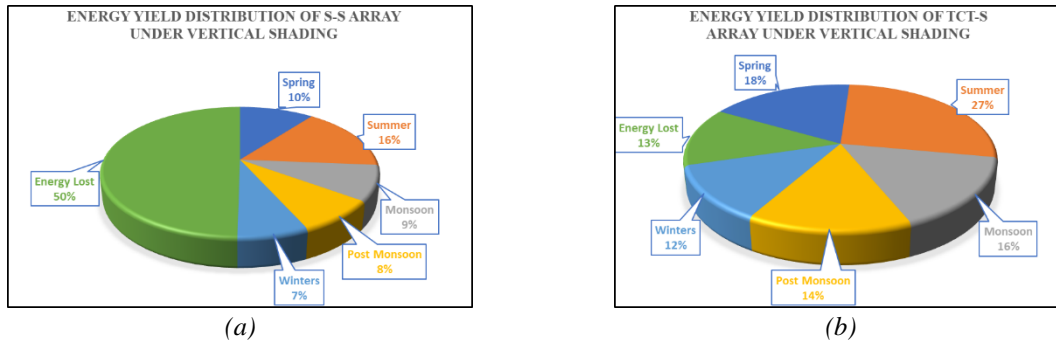


Figure 11. Percentage distribution of energy generated (%) and lost (%) in different seasons under the impact of vertical shading w.r.t the unshaded condition: (a) S-S and (b) TCT-S arrays.

The energy generated (%) and lost (%) in different seasons under the impact of vertical shading w.r.t the unshaded condition is depicted in Fig. 11. Under this shading condition, maximum energy generated by both the arrays is still in summer season. However, the energy generation is reduced to 16% for S-S and 27% for TCT-S array, in comparison to 31% generated in summer season under unshaded condition. Out of all the seasons, minimum energy is generated in winter, 7% for S-S and 12% for TCT-S in comparison to 14% energy generated in winter season under unshaded condition. The total energy loss in a year suffered by S-S array w.r.t the unshaded case is 50%, while TCT-S displays a much lower energy loss of only 13%.

### 3.4. Scenario-3: Square Shape Shading

#### 3.3.1. $P_{max}$ Matrix generated under square shading

The surface plot representing the variation of average  $P_{max}$  with different conditions of irradiance and temperature under shading scenario-3 is presented Fig.12. The obtained values of  $P_{max}$  for S-S array ranges from 51.6 W to 875.6 W, while for TCT-S array it is from 41 W to 963 W. The power output of S-S and TCT-S array at 1000 W/m<sup>2</sup> and 25 °C is 743.0 W and 823.7 W respectively.

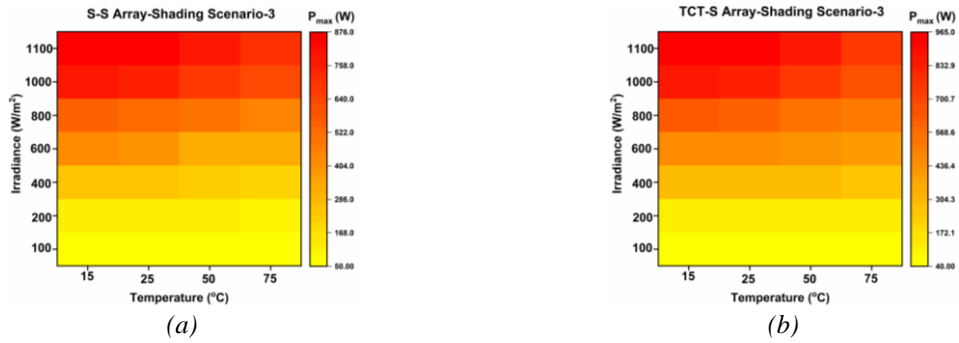


Figure 12. Surface plot showing the variation of  $P_{max}$  with irradiance and temperature under shading scenario-3 for (a) S-S and (b) TCT-S arrays.

### 3.4.2 Energy yield and DC performance ratio under square shaped shading

The seasonal energy yield and DC PR of both the arrays under the impact of square shaded shading is presented in Table 5. The total energy generated in one year by S-S and TCT-S array is 1042.5 kWh and 1202.0 kWh respectively. As seen from the results, seasonal energy yield and DC PR of the S-S is significantly reduced in comparison to the TCT-S array.

Table 5. Seasonal energy generation by array and DC performance ratio of 1kW each of S-S and TCT-S configuration under the impact of square shaped shading.

| Season       | Energy Generation under square shaped shading (kWh) |       | Performance Ratio under square shaped shading |       |
|--------------|---|-------|---|-------|
|              | S-S   | TCT-S | S-S   | TCT-S |
| Spring       | 216.8   | 247.2 | 0.661   | 0.745 |
| Summer       | 323.7   | 373.7 | 0.610   | 0.696 |
| Monsoon      | 190.9   | 218.4 | 0.629   | 0.708 |
| Post Monsoon | 169.6   | 197.5 | 0.630   | 0.725 |
| Winter       | 141.6   | 165.2 | 0.621   | 0.717 |

The seasonal energy loss for S-S array ranges from 72.3 kWh in winters (33.8% loss) to 155.6 kWh in summer (32.5% loss). On an average, S-S array displays an energy loss of 32.4%. TCT-S array displays reduced energy loss in all the seasons, ranging from 50.1 kWh in winters (23.3% loss) to 99.0 kWh in summer (20.9% loss). On an average, TCT-S array suffers a loss of 22.0% in a year.

The highest PR for both the arrays is obtained in spring season (0.661 for S-S and 0.745 for TCT-S) and least in summer (0.610 for S-S and 0.696 for TCT-S). The average yearly PR of S-S array falls to 0.630, whereas for TCT-S array it is 0.718.

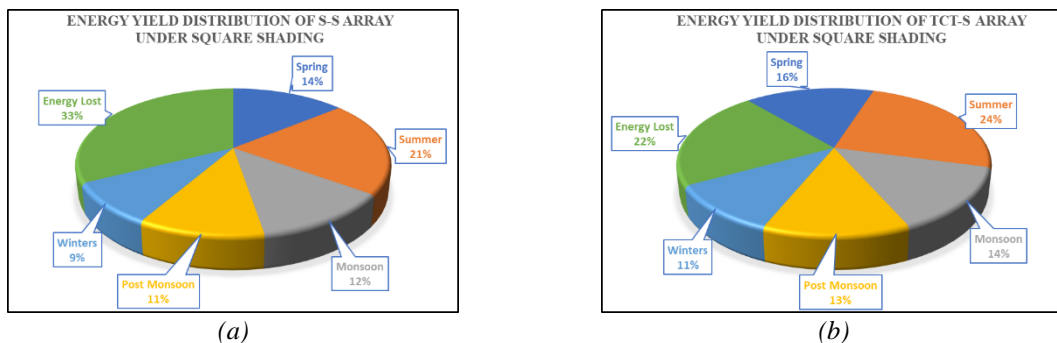


Figure 13. Percentage distribution of energy generated (%) and lost (%) in different seasons under the impact of square shape shading w.r.t the unshaded condition: (a) S-S and (b) TCT-S arrays.

The energy generated (%) and lost (%) in different seasons under the impact of square shaped shading w.r.t the unshaded condition is shown in Fig. 13. Under this shading condition, maximum energy generated in summer is reduced to 21% for S-S and 24% for TCT-S array, in comparison to 31%

generated under unshaded condition. Out of all the seasons, minimum energy is generated in winter, 9% for S-S and 11% for TCT-S in comparison to 14% energy generated in winter season under unshaded condition. The total energy loss in a year suffered by S-S array w.r.t the unshaded case is 33%, while for TCT-S it is 22 %.

The obtained results highlight the following points:

It is observed that under unshaded conditions, season induced variability impacts the energy generation of both S-S and TCT-S configuration of PV array equally. Energy yield is found to be maximum in summer (April-June) and least in winters (December-January). However, when the seasonal variation is combined with the impact of partial shading conditions, the energy yield and PR of the PV arrays is seriously affected, becomes more inconsistency and demonstrates dependence on the configuration of the array e.g., under the impact of shading scenario-2, S-S and TCT-S array demonstrated the energy loss of 10.3% & 2.7% in spring, 15.8% & 4.0% in summers, 8.7% & 2.4% in monsoon, 8.2% & 2.2% post monsoon and 6.9% & 1.8% in winter respectively. Generally, the minimum energy loss (%) is obtained in winters and maximum in summer. However, the energy loss (%) is not constant but varies with shading scenarios e.g., the energy loss exhibited by S-S array in summer under the impact of shading scenario-1,2 and 3 season is 18.2%, 15.85 and 10.1% respectively. When the configuration of the PV array is modified (TCT-S), this energy loss is reduced as it exhibits 13.9%, 4.0% and 6.8% energy generation loss in summers under impact of shading scenario-1,2 and 3 respectively.

The obtained PR also varies with seasons. It is observed that under non shaded as well as shaded conditions, highest monthly PR is obtained in spring season (Feb-Mar) and lowest in summer (Apr-Jun). This is possibly due to the low module temperature in spring and high temperature in summers, as the PR is significantly affected by module/array temperature. However, the traditional PR calculation doesn't take into account the array temperature which results in the seasonal variations, which can be removed by calculating a weather-corrected PR [36]. Also, another factor which affects PR is the seasonal spectral variation, which has not been considered in the present study. A detailed study taking into account the seasonal spectral variation with temperature corrected PR is the scope of the future work.

#### 4. CONCLUSION

In the presented work, the combined effect of seasonal variation and partial shading condition on the energy yield and DC performance ratio of the conventional and modified configuration of PV array has been investigated. Two different PV array configurations, S-S and TCT-S of PV array have been used. In this study, five seasons of India (spring, summer, monsoon, post monsoon and winter) and three commonly occurring PS scenarios - horizontal, vertical and square shaped have been considered.

Under unshaded conditions, different configurations of PV arrays have same seasonal energy yield and DC performance ratio. For any configuration of PV array, energy generation is impacted by the weather induced variability. Energy yield is maximum in the season which has maximum solar insolation and least in the season which has minimum solar insolation. The obtained results also substantiate that the combined effect of seasonal variation and shading condition leads to more pronounced fluctuation and deterioration in the energy yield of the PV array. Under the combined impact of seasonal variation and considered PSCs, the conventional array demonstrates more fluctuations in the energy generation. Under similar conditions, the modified PV array configuration has higher energy yield and less fluctuation in different seasons and thus outperforms the conventional one. The DC PR also exhibits seasonal variation. Highest temperature in summer results in lowest PR despite highest solar irradiance. It is also concluded that the configuration of PV array plays a significant role under partial shading conditions. The seasonal energy yield and PR of S-S array is seriously affected under any shading condition. TCT-S array under all shading scenarios has higher energy yield and PR than S-S array. However, the extent

of superiority of TCT-S over S-S array in terms of energy generation, energy loss suffered and PR depends majorly on the shading pattern.

The insight provided in this study are very significant which would help in the development of strategies and designing more efficient systems to optimize PV performance. The better seasonal energy yield of modified PV configuration and therefore its efficiency under PSCs, is achieved only by modifying the interconnection of PV cells of the conventional one. This design is simple to implement and doesn't strain the PV system with any additional cost burden. PV industry constantly endeavours to increase the PV energy generation while reducing cost at the same time. Therefore, the results of this study would be advantageous for the PV industry and solar project developers, and the end customers, especially living in congested urban areas where it is highly probable that for larger number of days in a year, the installed PV arrays gets partially shaded by nearby structures.

Our future scope of work includes detail study of long-term performance of the proposed array taking into account the seasonal spectral variation with temperature corrected performance ratio and dynamic shadow conditions.

### Acknowledgement

The author is grateful to administrative and technical staff at National Institute of Solar Energy (NISE), Gurgaon under Ministry of New and Renewable Energy (MNRE), Government of India, India for allowing to use the facilities for conducting this experimental study.

### Funding

This research did not receive any specific grant from funding agencies in the public, commercial, or not-for-profit sectors.

### REFERENCES

- [1] IRENA. *Renewable capacity statistics 2021*. Abu Dhabi: International Renewable Energy Agency; 2021. Available from: [https://www.irena.org/-/media/Files/IRENA/Agency/Publication/2021/Apr/IRENA\\_RE\\_Capacity\\_Statistics\\_2021.pdf](https://www.irena.org/-/media/Files/IRENA/Agency/Publication/2021/Apr/IRENA_RE_Capacity_Statistics_2021.pdf).
- [2] Ameer A, Berrada A, Bouaichi A, Loudiyi K. Long-term performance and degradation analysis of different PV modules under temperate climate. *Renewable Energy*. 2022;188:37-51. doi:10.1016/j.renene.2022.02.025.
- [3] Blakesley JC, Huld T, Müllejans H, Gracia-Amillo A, Friesen G, Betts TR, Hermann W. Accuracy, cost and sensitivity analysis of PV energy rating. *Solar Energy*. 2020;203:91-100. doi:10.1016/j.solener.2020.03.088.
- [4] Poddar S, Kay M, Prasad A, Evans JP, Bremner S. Changes in solar resource intermittency and reliability under Australia's future warmer climate. *Solar Energy*. 2023;266:112039. doi:10.1016/j.solener.2023.112039.
- [5] Katsumata N, Nakada Y, Minemoto T, Takakura H. Estimation of irradiance and outdoor performance of photovoltaic modules by meteorological data. *Solar Energy Materials and Solar Cells*. 2011;95(1):199-202. doi:10.1016/j.solmat.2010.01.019.
- [6] Wang H, Muñoz-García MA, Moreda GP, Alonso-García MC. Seasonal performance comparison of three grid connected photovoltaic systems based on different technologies operating under the same conditions. *Solar Energy*. 2017;144:798-807. doi:10.1016/j.solener.2017.02.006.
- [7] Phinikarides A, Makrides G, Zinsser B, Schubert M, Georghiou GE. Analysis of photovoltaic system performance time series: Seasonality and performance loss. *Renewable Energy*. 2015;77:51-63. doi:10.1016/j.renene.2014.11.091.
- [8] Vasisht MS, Srinivasan J, Ramasesha SK. Performance of solar photovoltaic installations: Effect of seasonal variations. *Solar Energy*. 2016;131:39-46. doi:10.1016/j.solener.2016.02.013.
- [9] Sevillano-Bendezú MA, Khenkin M, Nofuentes G, Casa J de la, Ulbrich C, Töfflinger JA. Predictability and interrelations of spectral indicators for PV performance in multiple latitudes and climates. *Solar Energy*. 2023;259:174-187. doi:10.1016/j.solener.2023.04.067.

- [10] Mustafa RJ, Gomaa MR, Al-Dhaifallah M, Rezk H. Environmental impacts on the performance of solar photovoltaic systems. *Sustainability (Switzerland)*. 2020;12:608. doi:10.3390/su12020608.
- [11] Kinsey GS, Riedel-Lyngskær NC, Miguel A, Boyd M, Braga M, Shou C, et al. Impact of measured spectrum variation on solar photovoltaic efficiencies worldwide. *Renewable Energy*. 2022;196:995-1016. doi:10.1016/j.renene.2022.07.011.
- [12] Dag HI, Buker MS. Performance evaluation and degradation assessment of crystalline silicon based photovoltaic rooftop technologies under outdoor conditions. *Renewable Energy*. 2020;156:1292-1300. doi:10.1016/j.renene.2019.11.141.
- [13] Ul-Abdin Z, Zeman M, Isabella O, Santbergen R. Investigating the annual performance of air-based collectors and novel bi-fluid based PV-thermal system. *Solar Energy*. 2024;276:112687. doi:10.1016/j.solener.2024.112687.
- [14] Kim C, Beltran L. Solar Constraints and Potential in Urban Residential Buildings. In: *Solar World Congress*; 08-12 November 2015; Daegu, Korea: International Solar Energy Society Conference Proceedings. doi:10.18086/swc.2015.08.03.
- [15] Calcabrini A, Weegink R, Manganiello P, Zeman M, Isabella O. Simulation study of the electrical yield of various PV module topologies in partially shaded urban scenarios. *Solar Energy*. 2021;225:726-733. doi:10.1016/j.solener.2021.07.061.
- [16] Agrawal N, Kapoor A, Gupta M. Monthly energy yield assessment of solar photovoltaic system under uniform irradiance and partial shaded condition. *Material Today Proceeding*. 2022;68:2699-2704. doi:10.1016/j.matpr.2022.06.240.
- [17] Brecl K, Bokalič M, Topič M. Annual energy losses due to partial shading in PV modules with cut wafer-based Si solar cells. *Renewable Energy*. 2021;168:195-203. doi:10.1016/j.renene.2020.12.059.
- [18] Agrawal N, Bora B, Rai S, Kapoor A, Gupta M. Performance Enhancement by Novel Hybrid PV Array Without and With Bypass Diode Under Partial Shaded Conditions: An Experimental Study. *International Journal of Renewable Energy Research*. 2021;11(4):1880-1891. doi:10.20508/ijrer.v11i4.12392.g8340.
- [19] Pendem SR, Mikkili S. Modelling and performance assessment of PV array topologies under partial shading conditions to mitigate the mismatching power losses. *Solar Energy*. 2018;160:303-321. doi:10.1016/j.solener.2017.12.010.
- [20] Bingöl O, Özkaya B. Analysis and comparison of different PV array configurations under partial shading conditions. *Solar Energy*. 2018;160:336-343. doi:10.1016/j.solener.2017.12.004.
- [21] Bana S, Saini RP. Experimental investigation on power output of different photovoltaic array configurations under uniform and partial shading scenarios. *Energy*. 2017;127:438-453. doi:10.1016/j.energy.2017.03.139.
- [22] Saeed F, Tauqeer HA, Gelani HE, Yousuf MH, Idrees A. Numerical modeling, simulation and evaluation of conventional and hybrid photovoltaic modules interconnection configurations under partial shading conditions. *EPJ Photovoltaics*. 2022;13:10. doi:10.1051/epjpv/2022004.
- [23] Agrawal N, Bora B, Kapoor A. Experimental investigations of fault tolerance due to shading in photovoltaic modules with different interconnected solar cell networks. *Solar Energy*. 2020;211:1239-1254. doi:10.1016/j.solener.2020.10.060.
- [24] Vunnam S, Vanitha Sri M, RamaKoteswara Rao A. An Optimal Triple-Series Parallel-Ladder Topology for Maximum Power Harvesting Under Partial Shading Conditions. *International Journal of Renewable Energy Research*. 2023;13(2):888-898. doi:10.20508/ijrer.v13i2.13885.g8762.
- [25] Yadav AS, Mukherjee V. Conventional and advanced PV array configurations to extract maximum power under partial shading conditions: A review. *Renewable Energy*. 2021;178:977-1005. doi:10.1016/j.renene.2021.06.029.
- [26] Fathy A, Yousri D, Sudhakar Babu T, Rezk H. Triple X Sudoku reconfiguration for alleviating shading effect on total-cross-tied PV array. *Renewable Energy*. 2023;204:593-604. doi:10.1016/j.renene.2023.01.046.
- [27] Horoufiany M, Ghandehari R. Optimization of the Sudoku based reconfiguration technique for PV arrays power enhancement under mutual shading conditions. *Solar Energy*. 2018;159:1037-1046. doi:10.1016/j.solener.2017.05.059.
- [28] Nihanth MSS, Ram JP, Pillai DS, Ghias AMY, Garg MA, Rajasekar N. Enhanced power production in PV arrays using a new skyscraper puzzle based one-time reconfiguration procedure under partial shade conditions (PSCs). *Solar Energy*. 2019;194:209-224. doi:10.1016/j.solener.2019.10.020.
- [29] Osmani K, Haddad A, Jaber H, Lemenand T, Castanier B, Ramadan M. Mitigating the effects of partial shading on PV system's performance through PV array reconfiguration: A review. *Thermal Science and Engineering Progress*. 2022;31:101280. doi:10.1016/j.tsep.2022.101280.
- [30] Mishra VL, Chauhan YK, Verma KS. Attenuation of shading loss using a novel solar array reconfigured topology under partial shading conditions. *Solar Energy*. 2024;274:112552. doi:10.1016/j.solener.2024.112552.
- [31] Agrawal N, Kapoor A, Gupta M. Estimation and comparison of annual energy yield of total cross tied-in-series and conventional PV array configuration under unshaded and commonly occurring partial shading

- conditions in urban areas. *International Journal of Renewable Energy Research*. 2023;13(1):463-473. doi:10.20508/ijrer.v13i1.13695.g8704.
- [32] Tamizhmani G, Paghasian K, Kuitche J, Gupta M, Sivasubramanian VG. *Solar ABCs Policy Recommendations: Module Power Rating Requirements*. United States: Solar America Boards for Codes and Standards; 2011. Available from: <http://www.solarabcs.org/powerratingpolicy>.
- [33] King DL, Boyson WE, Kratochvil JA. *Photovoltaic array performance model*. United States: Sandia National Laboratories; 2004. doi:10.2172/919131.
- [34] Durusoy B, Ozden T, Akinoglu BG. Solar irradiation on the rear surface of bifacial solar modules: a modeling approach. *Scientific Reports*. 2020;10:13300. doi:10.1038/s41598-020-70235-3.
- [35] IEC 61724: *Photovoltaic system performance monitoring - Guidelines for measurement, data exchange and analysis*. Switzerland: International Electrotechnical Commission; 1998.
- [36] Dierauf T, Growitz A, Kurtz S, Cruz JLB, Riley E, Hansen C. *Weather-Corrected Performance Ratio*. United States: National Renewable Energy Laboratory; 2013. Available from: <https://www.osti.gov/servlets/purl/1078057>.